

Mathematical modeling in quantification of [18F] FDG positron emission tomography images

Modelagem matemática na quantificação de imagens de tomografia por emissão de pósitrons com radiofármaco [18F] FDG

Nadine Skolaude Timm¹, Eliete Biasotto Hauser¹

¹Pontifícia Universidade Católica do Rio Grande do Sul, Porto Alegre, RS, Brasil

ABSTRACT

Techniques for locating and quantifying brain glucose metabolism using compartmental modeling by solving systems of differential equations ordinary require an input function (input function), $Ca(t)$. To avoid invasive procedures, such as collecting arterial blood samples, it is possible to obtain $Ca(t)$ of the first order ordinary differential equation $Cr'(t) = K1Ca(t) - K2Cr(t)$, where $Cr(t)$ describes the concentration of the radiopharmaceutical in a reference region. $Cr(t)$ is built from data obtained by processing images generated by positron emission tomography (PET) with radiotracers. In this work, the carotids were chosen as the reference region, and regression techniques were applied seeking to adjust the discrete activity curves (TAC) data obtained by PET imaging with the radiopharmaceutical fluorodeoxyglucose [18F]FDG. Aiming to find the same model type for all patients, the piecewise linear function proved to be adequate to describe four stages of the behavior of the $Cr(t)$ concentration: rapid growth and degrowth, intermediate and slow degrowths.

Keywords: Radiotracer; Positron emission tomography (PET); Reference region; Kinetic modeling

RESUMO

Técnicas de localização e quantificação do metabolismo de glicose cerebral utilizando modelagem compartimental via resolução de sistemas de equações diferenciais ordinárias requerem uma função de entrada (input function), $Ca(t)$. Para evitar procedimentos invasivos, como coleta de amostras de sangue arterial, é possível obter $Ca(t)$ da equação diferencial ordinária de primeira ordem $Cr'(t) = K1Ca(t) - K2Cr(t)$, onde $Cr(t)$ descreve a concentração do radiofármaco numa região de referência. $Cr(t)$ é construída a partir de dados obtidos pelo processamento de imagens geradas por tomografia por emissão de pósitrons (PET) com radiotraçadores. Neste trabalho, as carótidas foram escolhidas como região de referência, e técnicas de regressão foram aplicadas buscando ajustar os dados de curvas de atividades discretas (TAC) obtidas por meio de imagens PET com o radiofármaco fluorodeoxiglicose [18F] FDG. Com o objetivo de encontrar um mesmo tipo modelo para todos os pacientes, a função linear por partes

mostrou-se adequada para descrever quatro etapas do comportamento da concentração $C_r(t)$: crescimento e decrescimento rápidos, decrescimentos intermediário e lento.

Palavras-chave: Radiofármaco; Tomografia por emissão de pósitron (PET); Região de referência; Modelagem cinética

1 INTRODUCTION

There is a select population group, among people over eighty years old, in that some individuals show resistance to brain changes considered normal for age, with cognitive capacity similar to that of people twenty to thirty years younger. This group is defined as the super-elderly. On the other hand, there is a large number of people with Alzheimer's disease, persistent dementia and progressive. Using biomarkers, getting an early diagnosis can help in an attempt to prevent the disease from developing or reaching an advanced stage of degeneration (Borelli, 2019).

Positron emission tomography (PET) is an imaging technology that helps in the diagnosis and treatment of diseases, through the application of radiopharmaceuticals in the blood flow. To quantify the metabolic activity of the brain, the radiopharmaceutical [18F]2 – F luor2Deoxy – D – Glucose([18F]F DG) is used as a marker, which can aid in the detection of degenerative brain diseases, exhibiting the dynamics of the rate of Radiopharmaceutical glucose metabolism through PET imaging.

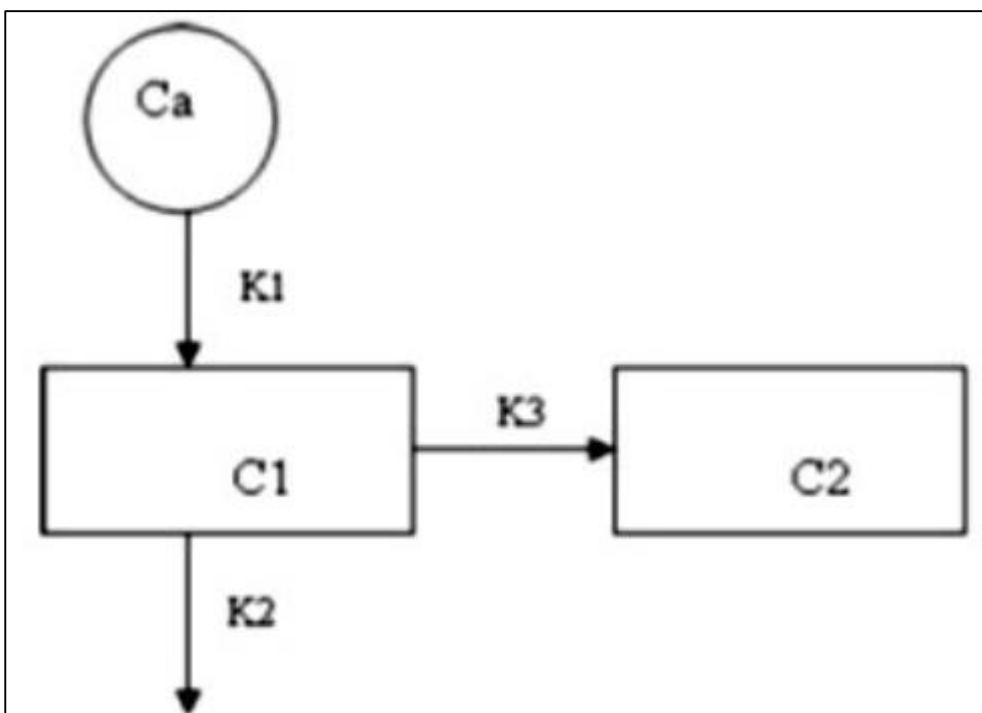
Mathematical modeling is used to describe the dynamics of [18F] FDG radiotracer through an irreversible two-compartment model, represented by a system of two differential equations, which depends on a input function, obtained from the concentration in arterial blood. Thus, the main objective of this work is to model activity curves (TAC) in a reference region, necessary in the construction of the input function. It should be noted that all data used in this study were obtained from the Superidosos project, developed at Rio Grande do Sul Brain Institute (InsCer).

2 METHODOLOGY

2.1 Irreversible two-compartment model

The two-compartment irreversible model, illustrated in Figure 1, is used to represent the change of state of the radiopharmaceutical [18F]FDG. Ca represents the arterial concentration of free FDG in plasma. The first compartment C1 represents the extravascular concentration of FDG in a target tissue, available for phosphorylation. The second compartment C2 represents the concentration of FDG which has undergone phosphorylation.

Figure 1 – FDG Two-Compartment Irreversible Model



Source: Hauser *et al.*, 2019

The mass conservation principle applied to the compartments allows build the mathematical representation of the irreversible two-compartment model of the FDG as a system of two first order ordinary differential equations expressed in Equation (1) below:

$$\begin{aligned}\frac{d}{dt} C_1(t) &= K_1 C_a(t) - (k_2 + k_3) C_1(t) \\ \frac{d}{dt} C_2(t) &= k_3 C_1(t)\end{aligned}\tag{1}$$

where, $C_a(t)$ is the input function, $C_1(t)$ e $C_2(t)$ are, respectively, the concentrations of FDG that first enters the free compartment C1 and then is irreversibly metabolized in the compartment C2, K_1 , k_2 and k_3 are the positive physiological transport constants that describe the inflow and the outflow. The initial concentrations in the two compartments are considered to be null, that is, $C_1(0) = 0$ and $C_2(0) = 0$.

The Laplace transform technique, as demonstrated in Hauser *et al.* (2019), allows quantifying the concentration in each compartment C1 and C2 through the system analytical solution (1), expressed by the convolution integrals:

$$\begin{aligned}C_1(t) &= K_1 e^{-(k_2+k_3)t} * C_a(t) = K_1 \int_0^t e^{-(k_2+k_3)(t-u)} C_a(u) du \\ C_2(t) &= k_3 * C_1(t) = k_3 \int_0^t C_1(u) du.\end{aligned}\tag{2}$$

In the construction of the input function $C_a(t)$ it is important to obtain a model that allows the calculation of the convolution integral (2).

2.2 Input Function from PET images

In order to avoid invasive procedures such as blood sample collection several studies are found in the literature proposing alternative techniques for construction of the input function (Hauser *et al.*, 2019; Hauser *et al.*, 2020). Considering a one-compartment model to describe the dynamics of FDG in a reference region, $C_r(t)$, where no phosphorylation occurs (a form of get the input function) the concentration of the marker in the blood plasma, $C_a(t)$ is obtained from the differential equation expressed in Equation (3):

$$\frac{d}{dt}C_r(t) = K'_1C_a(t) - k'_2C_r(t), \quad (3)$$

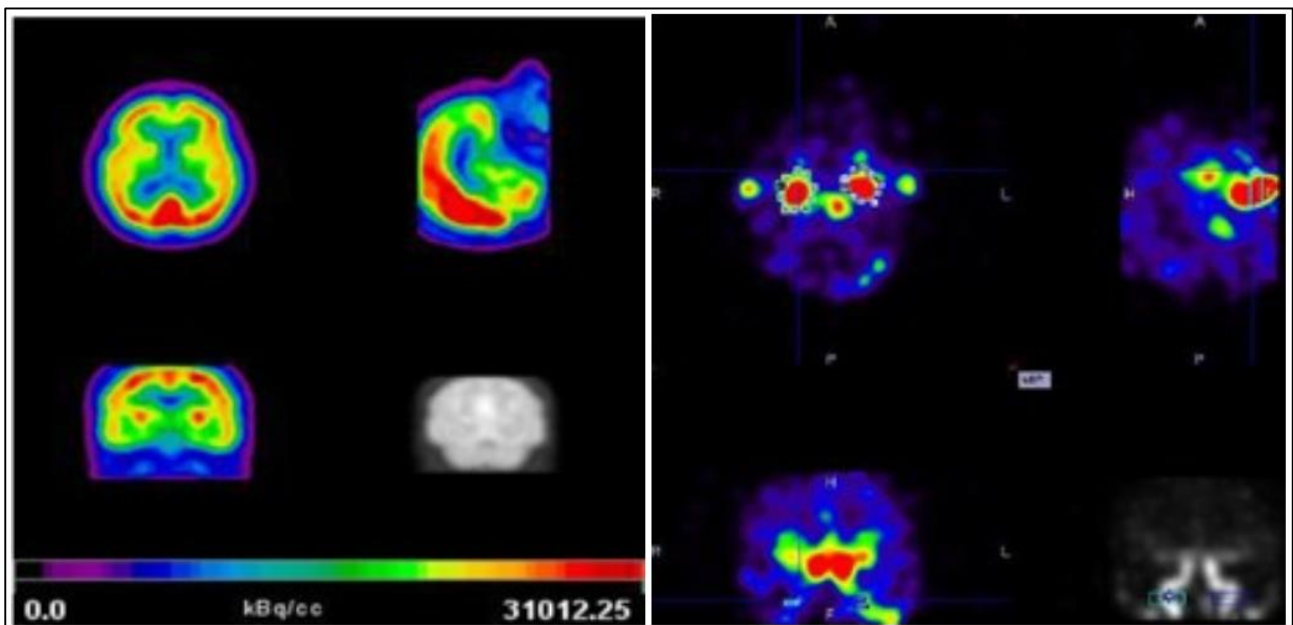
where $K'_1 > 0$ and $k'_2 > 0$ are the shipping fees. The main objective of this work is to determine $C_r(t)$ from PET image processing with FDG, a reverse engineering technique.

3 RESULTS

FDG PET CT scans were performed in three volunteer patients participants of the Superidosos project developed at InsCer. Images were obtained on GE Healthcare Discovery DiscoveryD 600 equipment, protocol observed pre-set doctor. Data were collected in DICOM format and then later processed using the PMOD biomedical quantification *software* (PMOD Technologies LLC, Zurich).

The reference regions (right carotid and left) and created a Volume of Interest (VOI), as shown in Figure 2.

Figure 2 – FDG PET axial, coronal and sagittal orientation and Bilateral Carotid VOI

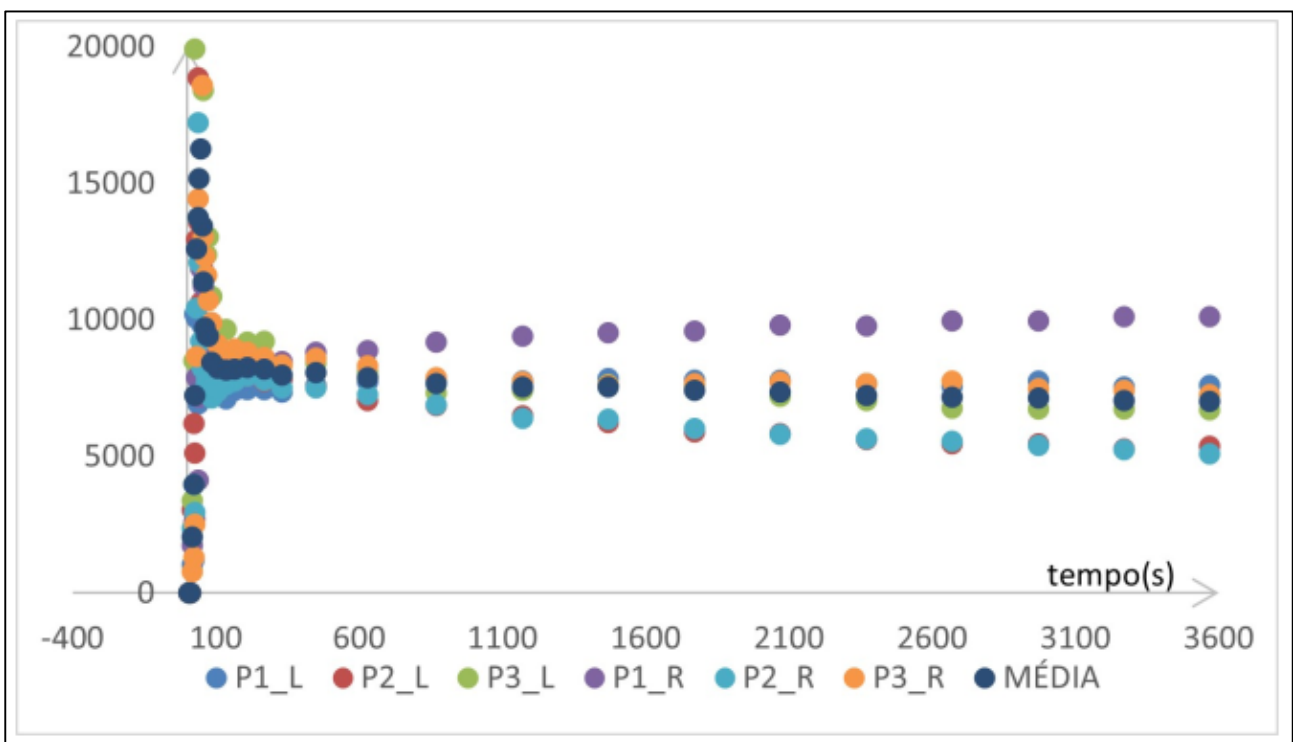


Source: Oliveira, 2019

For the three patients, the activity curves were defined in the created VOIS (TAC), a discrete set of points graphically represented in Figure 3. From the PET image, the activity curves (TAC) are obtained, a discrete and finite set of FDG points in the VOI, as shown in Figure 3.

Different functions are suitable for different patients when applied non-linear regression techniques (Hauser *et al.*, 2019; Hauser *et al.*, 2020). So, in order to find the same model type for all patients, the piecewise linear function was adequate to describe four steps of concentration behavior: very fast growth, fast degrowth, intermediate degrowth and slow degrowth.

Figure 3 – Discret TAC



Source: Of the author

The time interval $[0, 3570]$, PET image acquisition time, was subdivided into four sub-intervals: $[0, 47.5]$, $[47.5, 85]$, $[85, 1170]$ and $[1170, 3570]$, and linear regression was applied. The linear model $Cr(t) = At + B$ proved to be adequate for all four time sub-intervals considered, with few exceptions.

Table 1 shows the values obtained for A and B, for $t \in [0; 47.5]$. The lowest Pearson correlation coefficient was 0.6811 and occurred for P2-R.

Table 1 – Parameters A e B, $t \in [0; 47,5]$

| Carotid | A | B | R |
|----------------|----------|----------|----------|
| P1-L | 278,2 | -2222,7 | 0,7143 |
| P1-R | 253,13 | -2657,4 | 0,8056 |
| P2-L | 391,15 | -2818,2 | 0,7132 |
| P2-R | 350,71 | -3067,9 | 0,6811 |
| P3-L | 841,55 | -7556,4 | 0,914 |
| P3-R | 623,93 | -8844 | 0,8414 |

Table 2 shows the values obtained for A and B, for $t \in [47.5 ; 85]$. The lowest Pearson correction coefficient was 0.6774 and occurred for P2-L.

Table 2 – Parameters A e B, $t \in [47,5 ; 85]$

| Carotid | A | B | R |
|----------------|----------|----------|----------|
| P1-L | -65,772 | 12812 | 0,7944 |
| P1-R | -122,68 | 17743 | 0,8562 |
| P2-L | -63,849 | 12618 | 0,6774 |
| P2-R | -44,786 | 10892 | 0,7363 |
| P3-L | -482,86 | 48306 | 0,735 |
| P3-R | -531,13 | 47144 | 0,8838 |

Table 3 – Parameters A e B, $t \in [85 ; 1170]$

| Carotid | A | B | R |
|----------------|----------|----------|----------|
| P1-L | -0,2294 | 7393,2 | 0,6307 |
| P1-R | -1,0848 | 7993,5 | 0,8959 |
| P2-L | -1,3616 | 8084 | 0,8561 |
| P2-R | -1,0182 | 7800,4 | 0,6507 |
| P3-L | -2,514 | 9817,9 | 0,7403 |
| P3-R | -1,4627 | 9242,6 | 0,7377 |

Table 4 shows the values obtained for A and B, for $t \in [1170 ; 3570]$. The lowest Pearson correction coefficient was 0.4944 and occurred for P1-L.

Table 4 – Parameters A e B, t ∈ [1170 ; 3570]

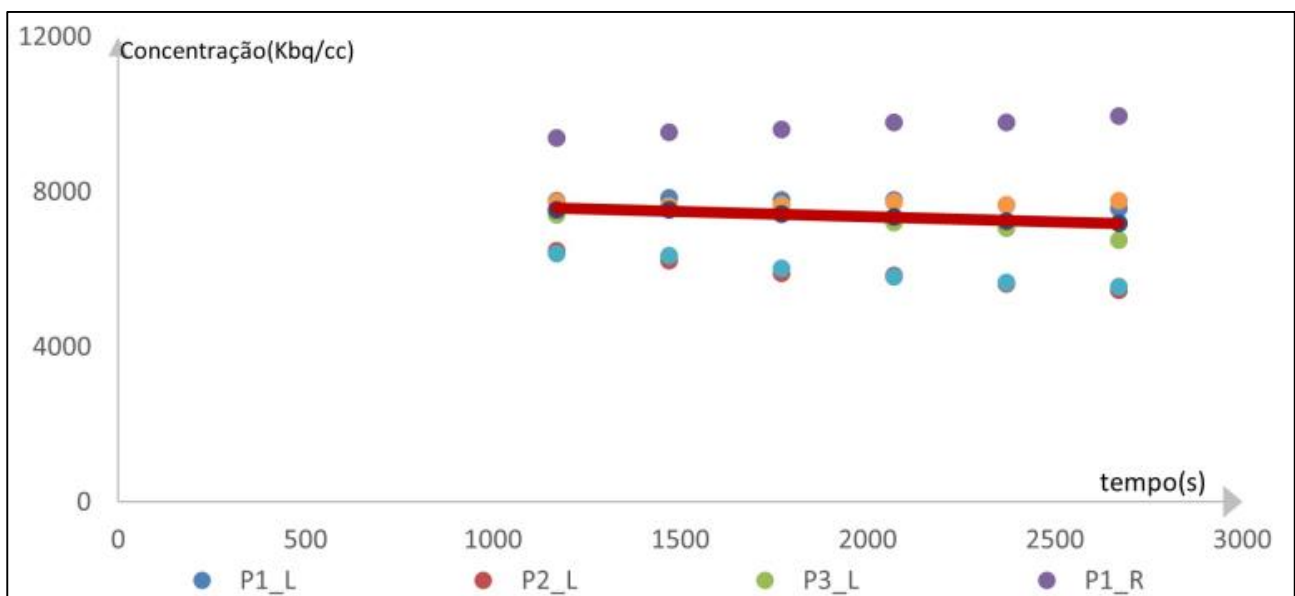
| Carotid | A | B | R |
|---------|---------|--------|--------|
| P1-L | -0,1157 | 7987,7 | 0,4944 |
| P1-R | -0,2767 | 9168,4 | 0,9254 |
| P2-L | -0,477 | 6871,6 | 0,9124 |
| P2-R | -0,5598 | 7058,9 | 0,9804 |
| P3-L | -0,4263 | 8109,4 | 0,8289 |
| P3-R | -0,1512 | 7956,2 | 0,5531 |

In an attempt to build a single Cr(t) for all patients it was considered the mean value of the concentrations in Figure 1, at each time. It might be convenient in diagnosing Alzheimer's to consider the time interval [1200, 2700]. In this time interval, with $R^2 = 0:9598$, the linear model expressed in the Equation (4).

$$C_r(t) = -0,2576 t + 7878,9 \quad (4)$$

and illustrated graphically in Figure 4.

Figure 4 – Discrete TAC and Cr(t) considering average values for t in [1200; 2700]



Source: of the author

4 FINAL CONSIDERATIONS

From the processing of PET images, in this work a reverse engineering technique to non-invasively determine concentration $Cr(t)$ of the [18F]FDG radiopharmaceutical in a reference region (carotids), necessary for solve an irreversible two-compartment model that describes the metabolism of glucose in Alzheimer's dementia. The piecewise linear function proved to be adequate for the three patients considered and described four stages of the behavior of the concentration: very fast growth, fast degrowth, degrowth intermediate and slow degrowth. Also, in search of a single $Cr(t)$ for all the patients, the linear model proved to be adequate when considering the mean value of the concentrations at each time.

THANKS

This study was possible due to the teamwork of all members of the Superidosos project, which was partially supported by CNPq, project number 403029/2016-3 and FAPERGS, project number 27971.414.15498.22062017.

REFERENCES

- BORELLI, W. V. (2019). **Correlação Entre Neuroimagem Molecular, Estrutural e Funcional em Superidosos**. 143 f. Thesis (Doctorate) Programa de Pós-Graduação de Medicina e Ciências da Saúde da Pontifícia Universidade Católica do Rio Grande do Sul. Porto alegre.
- HAUSER, E. B., VENTURINI, G. T., GREGGIO, S., BORELLI, W. V., COSTA, J. C. (2019). Carotid arterial input function as an inverse problem in kinetic modeling of [18F]-fluoro-2-deoxy-D-glucose (FDG). **Computer Methods in Biomechanics and Biomedical Engineering: Imaging & Visualization**, 8, 2168-2171.
- HAUSER, E. B., BORELLI, W. V., COSTA, J. C. (2020). Biomechanical Model Improving Alzheimer's Disease. In: Redha Tair, editor. **Recent Advances in Biomechanics** 77-91. Intech Open.
- OLIVEIRA, F. (2019). **Modelo Logístico para Descrever as Atividades de Curvas Discretas Obtidas de Imagens PET com Radiofármaco [18F]FDG num Volume de Interesse das**

Carótidas. 28 f. Dissertation (Lato sensu) Pontifícia Universidade Católica do Rio Grande do Sul Porto Alegre.

CONTRIBUIÇÃO DE AUTORIA

1 – Nadine Skolaude Timm

Undergraduate student in Chemical Engineering, Pontifical Catholic University of Rio Grande do Sul, PUCRS. School of Technology

<https://orcid.org/0000-0002-4210-2174> - nadine.timm@acad.pucrs.br

Contribuição: Conceptualization | Data curation | Formal Analysis | Investigation | Methodology | Project administration | Resources | Software | Supervision | Validation | Visualization | Writing – original draft | Writing – review & editing

2 – Eliete Biasotto Hauser

PhD in Applied Mathematics, PhD in Mechanical Engineering, Master in Mathematics, Pontifical Catholic University of Rio Grande do Sul, PUCRS. School of Technology

<https://orcid.org/0000-0001-7494-2461> - eliete@pucrs.br

Contribuição: Conceptualization | Data curation | Formal Analysis | Investigation | Methodology | Project administration | Resources | Software | Supervision | Validation | Visualization | Writing – original draft | Writing – review & editing

Como citar este artigo

TIMM, N.S.; HAUSER, E.B. Mathematical modeling in quantification of [18F] FDG positron emission tomography images. **Ciência e Natura**, Santa Maria, v. 43, Ed. Esp. X ERMAC RS, e6, p. 1-10, 2021. DOI 10.5902/2179460X66979. Disponível em: <https://doi.org/10.5902/2179460X66979>. Acesso em: 5 nov. 2021.